Astron. Astrophys. 330, 612–618 (1998)

ASTRONOMY AND ASTROPHYSICS

Rapid expansion in the VLBI structure of LSI+61°303

M. Peracaula[1,2], **D.C. Gabuzda**[3], **and A.R. Taylor**[1]

[1] Department of Physics and Astronomy, University of Calgary, 2500 University Dr. NW, Calgary, AB T2N 1N4 Canada
[2] Departament d'Astronomia i Meteorologia, Universitat de Barcelona, Av. Diagonal 647, E-08028 Barcelona, Spain
[3] Astro Space Center, Lebedev Physical Institute, 53 Leninsky Pr., 117924 Moscow, Russia

Received 28 January 1997 / Accepted 18 September 1997

Abstract. We present the results of global VLBI observations at 6 cm wavelength of the X-ray binary LSI+61°303 made at epoch 1992.4. During the course of our 24 hour VLBI observing session, the integrated flux measured simultaneously with the VLA indicated that the source was experiencing a minor flare, with the total flux rising and falling by $\sim$ 12 mJy. Our VLBI observations indicate that this brightening occurred on milli-arcsecond scales, and was accompanied by an increase of the compact radio structure size with velocity $\sim 0.06c$, which appeared to decelerate rapidly upon reaching a dimension of about 4 AU.

Key words: stars: individual: LSI+61°303 – stars: variables – stars: emission-line, Be – radio continuum: stars – X-rays: stars

1. Introduction

The X-ray binary LSI+61°303 was discovered to be a radio source by Gregory & Taylor (1978). The source also emits at infrared through X-ray wavelengths (Waters et al. 1988; Mendelson & Mazeh 1989; Bignami et al. 1981; Taylor et al. 1995), and probably at γ-ray wavelengths as well (Hermsem et al. 1977; Fichtel et al. 1994). One of the most unusual aspects of the radio emission of LSI+61°303 is that it exhibits regular nonthermal outbursts with period P=26.5 days (Taylor & Gregory 1982), which corresponds to the orbital period of the binary system (Hutchings & Crampton 1981). This 26.5-day periodicity has also been seen in the optical (Mendelson & Mazeh 1994) and infrared (Paredes et al. 1994) variations of LSI+61°303.

The radio emission of LSI+61°303 is consistent with that expected for synchrotron radiation from relativistic electrons. Its flux level between outbursts is typically $\sim 20-40$ mJy, and reaches $\sim 60-320$ mJy during outburst. A possible four year modulation of this variability in the strength of the outburst peak has been proposed by Gregory et al. 1989 and Paredes et al. 1990.

Send offprint requests to: M. Peracaula

X-ray binaries are usually thought to consist of a neutron star or black hole accreting matter from a companion star. The companion star of LSI+61°303 is a rapidly rotating B0-B0.5 main sequence star showing emission lines (Hutchings & Crampton 1981). A number of models have been proposed to explain the periodic radio outbursts in LSI+61°303; it is not yet clear which of these is closest to describing the actual physical processes in the source. One possibility is that the accretion rate near periastron becomes supercritical, giving rise to the ejection of a cloud of relativistic electrons, which then expands along the rotation axis of the accretion disk (Taylor & Gregory 1984). It has also been suggested (Maraschi & Treves 1981) that the companion star is a young pulsar with a relativistic wind, and that relativistic (synchrotron) electrons are produced at the interaction front between the Be star and the pulsar wind. Verstrand (1983) has also proposed that the companion is a pulsar that is enshrouded in matter and produces γ rays; in this model, relativistic electrons are generated by pair production and by Compton scattering of thermal electrons.

Taylor et al. (1992) and Massi et al. (1993) have used VLBI observations to indirectly infer (assuming a given epoch for the onset of the outburst) expansion velocities on milli-arcsecond scales of the order of hundreds of km/sec; this is roughly two orders of magnitude lower than appears to be typical of other X-ray binaries studied with VLBI, which have tended to have velocities $\sim 0.15-0.30c$ (Cyg X-3: Molnar et al. 1988; SS 433: Hjellming & Johnston 1981), or even greater (GRS 1915+115, $\sim 0.9c$: Mirabel & Rodríguez 1994). We present the results of new VLBI observations of the source carried out during a 24 hour period at phase 0.4 (from 0.38–0.42) for the major outburst cycle. The usual phase for strong outburst peaks is 0.6, but relatively weak peaks have been observed to occur at various phases from 0.4–1.0 (Paredes et al. 1990). Thus, based on the total flux during our observations ($\sim 25-35$ mJy), it is clear that the radio emission was essentially quiescent, but we cannot be sure where our observing epoch falls relative to the nearest outburst peak. Although astrometric VLBI observations of LSI+61°303 by Lestrade et al. (1988) made when the radio emission was quiescent have been used to derive estimates of

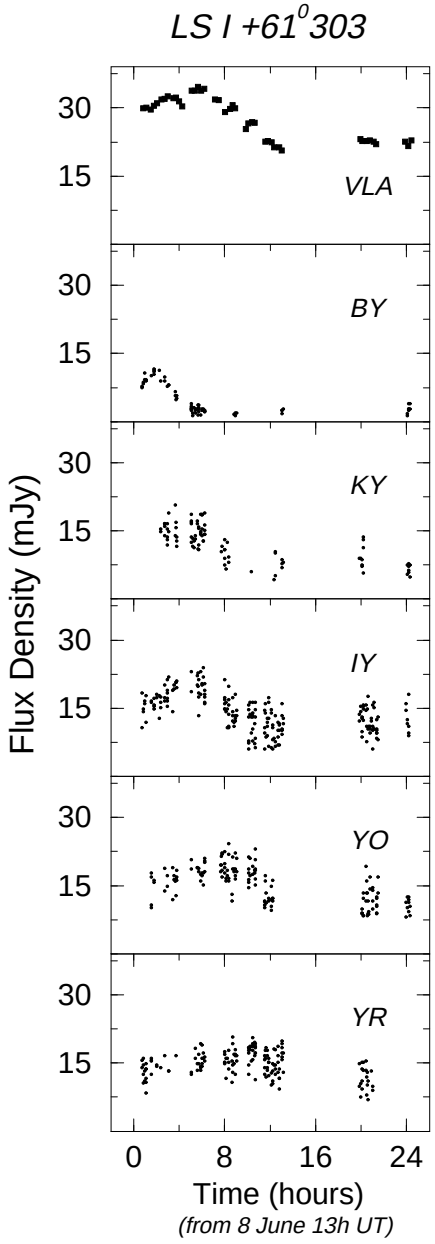

Fig. 1. Flux measured by the VLA and on the most sensitive baselines of our VLB interferometer (those involving the VLA)

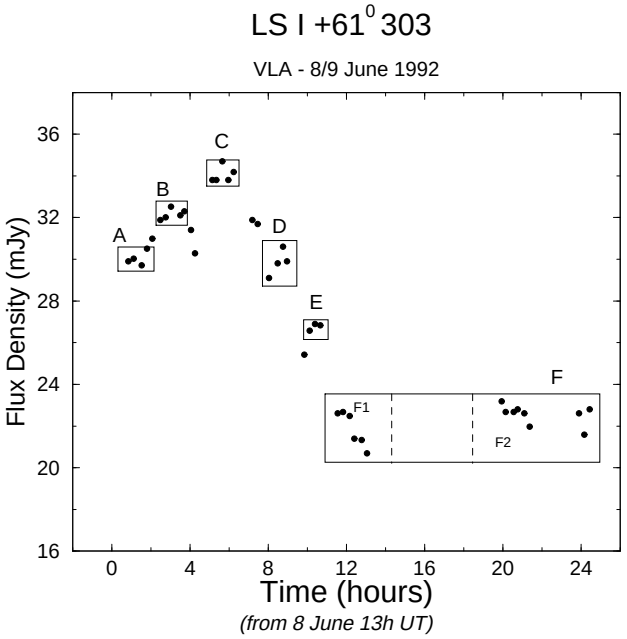

Fig. 2. Flux variations measured by the VLA during our VLB experiment, with boxes showing the different datasets used to make individual VLBI images during periods when the flux was roughly constant

Table 1. Antennas used

Antenna	Location	Diameter (m)
Effelsberg	Bonn, Germany	100
Haystack	Westford, Massachusetts	37
North Liberty	North Liberty, Iowa	25
Phased VLA	Socorro, New Mexico	$\sqrt{27} \times 25$
OVRO	Big Pine, California	25
Brewster	Brewster, Washington	25

the source size, the results presented here are the first VLBI images of the quiescent emission.

2. Observations

We present here results of the analysis of VLBI images of LSI+61°303 derived from observations taken at epoch 1992.4 at 6 cm wavelength using the antennas listed in Table 1. The data were recorded using the Mk III VLBI system and correlated on the Mk IIIA correlator at Haystack Observatory. All antennas recorded both the RCP and LCP signals incident from the radio source, and both RR and LL correlations were made and used in our images. Hybrid maps of the distribution of total intensity I were made using a self-calibration algorithm similar to that described by Cornwell & Wilkinson (1981) in the Brandeis VLBI package (Roberts et al. 1994).

One of the antennas in our VLB array was the phased Very Large Array. In addition to using the VLA as a VLBI element, we processed the VLA observations separately to derive integrated flux measurements during the VLBI experiment. This provided essentially continuous monitoring of the flux of LSI+61°303 during the VLBI observations. The flux calibration of the VLA data was done using observations of the standard flux calibrators 3C48 and 3C286. The phase calibration of the VLA data for LSI+61°303 was done using the nearby calibrator 0228+673, which was observed prior to each observation of LSI+61°303. With the VLA data we also obtained an image of the source using the AIPS package of NRAO. This VLA map shows an unresolved source that provides an upper limit of 2" for its size.

3. Results

Measurements made with the VLA during our VLBI observations show that LSI+61°303 was experiencing a "mini-flare"

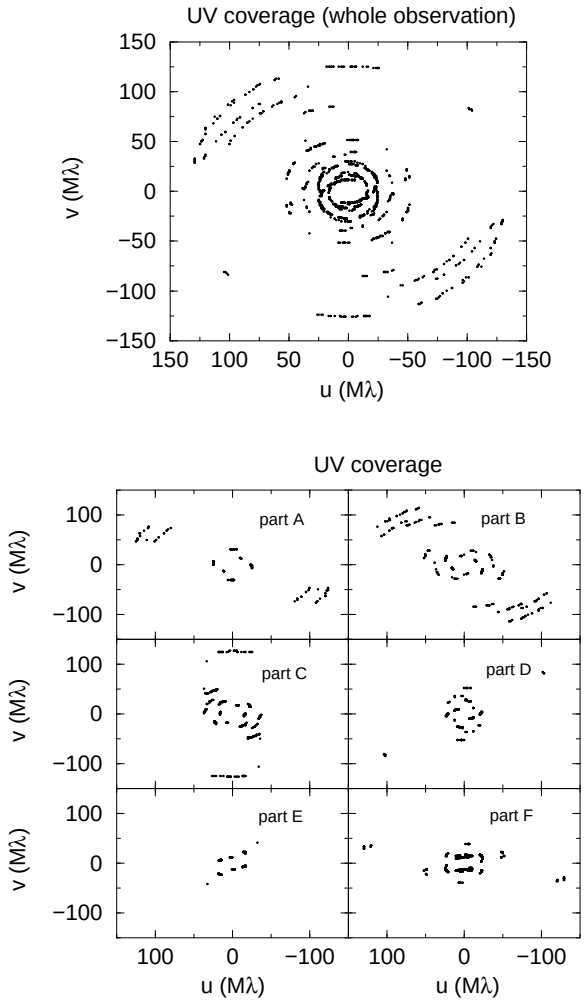

Fig. 3. u-v coverages for the entire VLB dataset, and for the separate datasets A–F

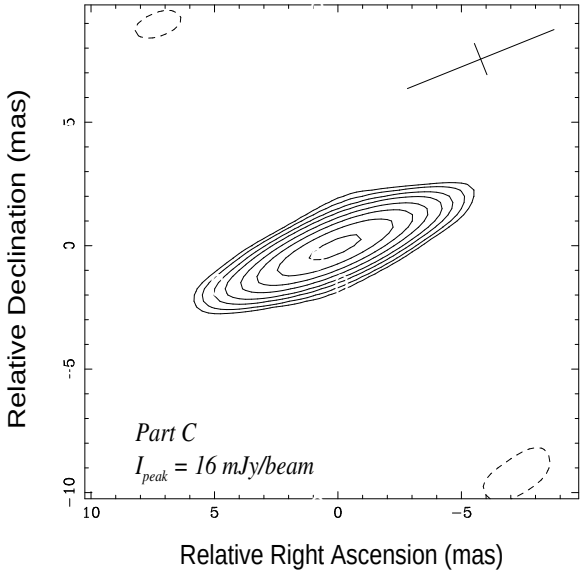

Fig. 4. Hybrid map for dataset C. The antenna beam is shown as a cross in the top right corner and the contours go up in multiples of the square root of 2; the bottom contour is 8% of the peak.

during our observing time, with the total flux rising from ∼30 mJy to ∼35 mJy and then falling to ∼22 mJy, as shown in the top panel of Fig. 1. This represents a substantial variation in the flux density, of the order of $50 - 60\%$. The amplitudes for the VLBI baselines involving VLA are also plotted in this figure. As can be seen, the amplitudes for individual VLBI baselines appear to track the integrated variations measured with the VLA, suggesting that the variations occurred on VLBI scales. The amplitudes for increasing shorter baselines begin to decay successively later, indicative of expansion in the size of the compact radio structure. This kind of "mini-flares" have been seen in many observations of LSI+61°303 light curves both between and during the actual outbursts (superposed onto the general trend of the flux density rise and decay). Taylor & Gregory (1984) interpret them as successive events of luminosity-driven shocks (LDSs) which produce relativistic particles. Peracaula et al. (1997) have observed a quasi-periodic modulation of about 1.4 hours superposed onto some of these small amplitude radio flares when they occur near the outburst peak.

In order to minimize the effect of time variations on our VLBI images, as well as to study the nature of the mini-flare, we divided the VLBI data into five time ranges, during each of which the total source flux as indicated by the VLA observations was roughly constant. These time ranges, which we refer to as "A-F", are shown in Fig. 2 and they correspond to the flare rise (A and B), the flare maximum (C), the flare decay (D and E), and the post-flare state (F). Figure 2 shows that some scans do not fall into any of the boxes indicated. These few scans were not used in our analysis because their integrated fluxes were substantially different from surrounding regions on the integrated flux curve, but there were not enough data for an independent analysis.

The u-v coverages for the entire data set and for each individual time range are shown in Fig. 3. It is important to notice that the visibilities are distributed along a preferential direction that is rather different for each part (due to the shortness of their sampling time range, the hour angle covered by the rotation is quite narrow). Therefore, the resolution we have for the images is highly concentrated in one direction which is different for each part. Figure 3 also shows, there are long (trans-Atlantic) baselines for all parts except part E.

We obtained images for periods A, B, C, and D through the hybrid mapping process. As an example of our results we show in Fig. 4 the map obtained for part C. As it can be seen the source did not show a complex structure during the observing run. There were not enough complete triangles of data in parts E and F for the hybrid mapping process to reconstruct the data phases, and so no maps were obtained for these time ranges. In addition, the data were insufficient for us to use amplitude self-calibration during the hybrid mapping.

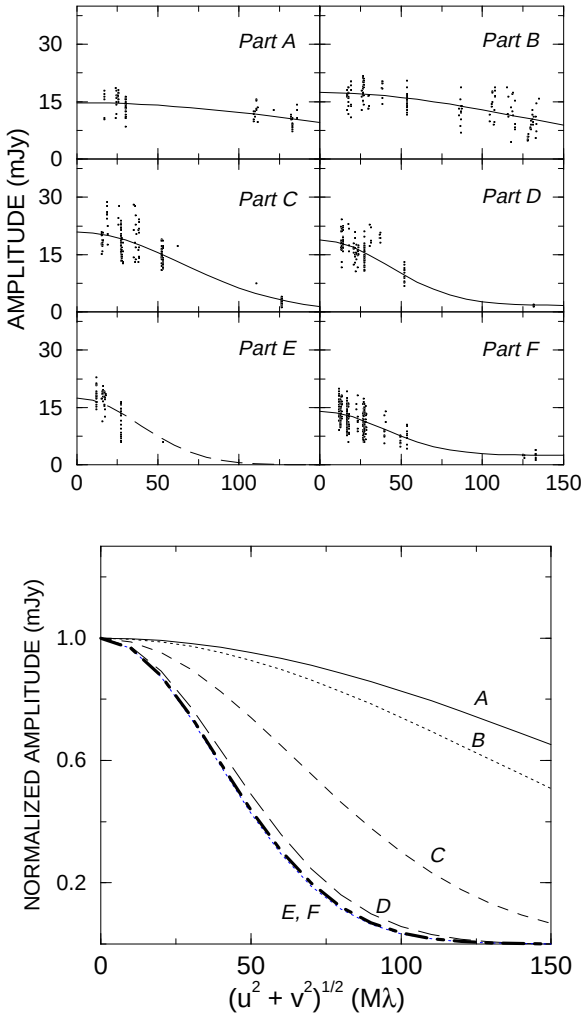

Fig. 5. Plots of the visibility amplitudes for each dataset (A–F) as a function of u-v distance. The solid lines overlaid represent circular gaussian + point (A,B,C, D, F) fits to these amplitudes. The fit for part E is a single circular gaussian represented in dashed lines because of its larger uncertainty due to the lack of data at large u-v distances. The bottom panel shows an overlay of the normalized gaussian component of the fits for the different datasets, clearly showing a tendency for the width of the gaussian in the visibility plane to decrease with time, corresponding to an increase of the source size with time. The increase is rapid up to part D, then stops abruptly.

Plots of the visibility amplitudes as a function of u-v distance are shown in Fig. 5. As can be seen from these plots, LSI+61°303 is only marginally resolved in part A, but quickly becomes obviously well resolved. Models for the source structure were investigated by fitting the visibilities that come from the hybrid mapping process using a variety of models, as described by Roberts et al. (1987) and Gabuzda et al. (1989). The limited u-v coverage for the individual parts prevents us from determining whether there is elongated structure along a well-defined direction during our observations; in particular, we cannot say if at our epoch LSI+61°303 is extended along structural

Table 2. Gaussian fit to the VLBI amplitudes

	Time	S_{VLA} (mJy)	S_g (mJy)	S_p (mJy)	S_{tot} (mJy)	FWHM (mas)
A	$0^d\ 14.4^h$	30.0±0.4	14.3	0.8	15.1±1.0	0.5 ± 0.1
B	$0^d\ 16.0^h$	32.2±0.3	16.6	1.0	17.6±0.7	0.6 ± 0.1
C	$0^d\ 18.7^h$	34.9±0.4	20.2	1.1	21.3±0.9	1.2 ± 0.2
D	$0^d\ 21.7^h$	29.9±0.6	17.1	1.7	18.8±1.0	1.8 ± 0.2
E*	$0^d\ 23.4^h$	26.9±0.2	17.5	-	17.5±0.8	2.0 ± 0.4
F_1	$1^d\ 01.3^h$	21.9±0.9	12.0	2.4	14.4±0.9	1.9 ± 0.2
F_2	$1^d\ 11.1^h$	22.6±0.5	11.3	2.6	13.9±0.5	2.1 ± 0.2

*Gaussian+point fit not possible due to lack of data at large u-v distances

position angle $\sim 45°$, as in the image by Massi et al. (1993), taken close to a main outburst maximum.

We concluded that a reasonable approach to investigating the behavior of of the radio source during the course of our VLB observations was to fit a single circular gaussian component to the data for each time range in order to obtain an estimate of the size for each part. Because the quantity and quality of phase data for the different time ranges was rather non-uniform, we decided that fitting the visibility amplitudes was the best way to obtains models for all the parts in a systematic way. The amplitude data for parts A, B, and C are very well fit both by a single circular gaussian component or a weak point plus a circular gaussian component, while parts D and F require both components (a point and a circular gaussian) for a satisfactory fit.

For part E it was not possible to determine the presence or the flux level of the weak point component present in parts D and F, since the absence of long baselines for this time range (see Fig. 3) does not allow us to determine the constant level added to the gaussian fit in the u-v plane. Although we were able to obtain circular gaussian + point fits for parts A, B, and C, in these cases, the point component was quite weak; the fits are quite similar to those for a circular gaussian alone. We shall consider the circular gaussian + point fits for these three parts, in order to treat the data for the different times as uniformly as possible. The resulting fits are shown in Fig. 5 by the solid lines superposed on the data for each individual part. Due to its separation in time, and in order to see if there had been some evolution, we considered the datasets labeled F1 and F2 in Fig. 1 independently, and confirmed that the parameters fit for both parts were practically the same; therefore, parts F1 and F2 are shown together as part "F" in Fig. 5. A summary of the model properties is given in Table 2. In all cases where it was possible to obtain circular gaussian fits using phase information as well (parts A, B, C, and D), these were fully consistent with the amplitude fits.

4. Discussion

4.1. Evolution of the VLBI structure

We may investigate the evolution of the VLBI structure in LSI+61°303 during this mini-flare by comparing the models obtained for each time period. Figure 6 shows a plot of the integrated flux measured by the VLA and the total flux from the

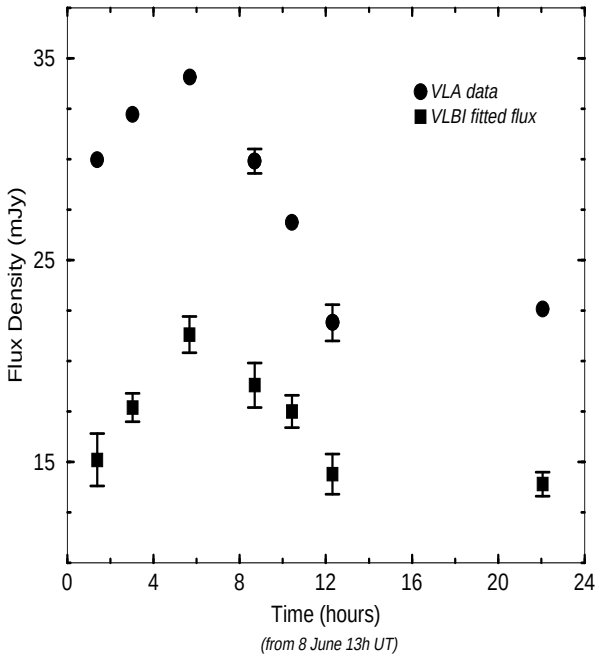

Fig. 6. Integrated flux measured by the VLA and the total flux contained in our VLBI models. The variations in the total milli-arcsecond-scale flux track fairly well the variations measured by the VLA, indicating that these variations occurred on the scales measured by our VLB interferometer

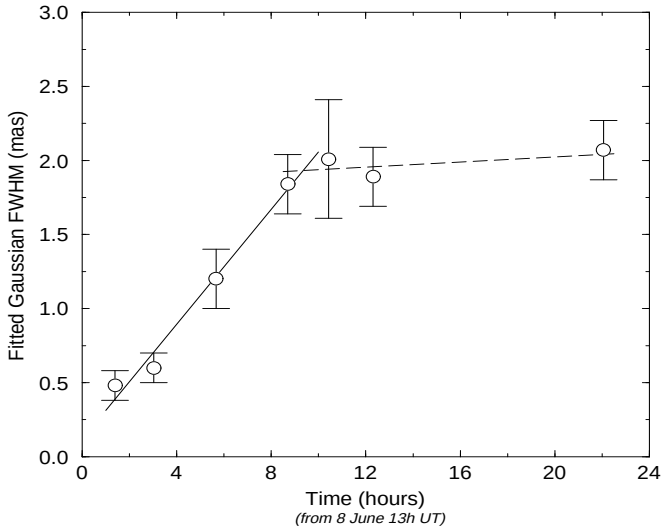

Fig. 7. Size of the circular gaussian components from Table 2 as a function of time. During the mini-flare, the source size grows linearly with $v = (0.06 \pm 0.01)c$ up to parts D-E (the mini-flare decline), then stays constant for the remainder of our observing period

VLBI models in Table 2. As can be seen, the variation in the total fluxes derived from the amplitude fits track the integrated variations fairly well, indicating that the variations measured by the VLA occurred on milli-arcsecond scales. While the fluxes for the gaussian components rise and fall with the VLA fluxes, those for the weak VLBI point component monotonically increase during the mini-flare. It is not clear if this is due to (1) an actual growth in the strength of this component, or (2) to the fact that it becomes more visible as the gaussian component expands. The fact that in many light curves of LSI+61°303 with short sampling time intervals several consecutive or even overlapped mini-flares are seen suggests us that possibility (1) could be due to the onset of a subsequent mini-flare.

In the bottom panel of Fig. 5, we have plotted together the gaussian visibility components for each fit normalized to peak amplitude 1. This figure clearly shows a decrease in the gaussian FWHM in the visibility plane (corresponding to an increase of the source size in the image plane) with time for parts A–D. The source size stays roughly constant soon after the peak of the miniflare during parts D–F.

Figure 7 shows a plot of circular gaussian size versus time, where 0^h is arbitrarily set to correspond to the beginning of the observations. The model results for parts F1 and F2 are plotted separately here in order to more clearly show the evolution of the source structure after the burst maximum. This plot indicates that during the flare up to part D, the compact radio source expanded uniformly in time; a linear regression fit indicates the velocity to be $v = (0.06 \pm 0.01)c$ for a distance of about 2 kpc. This is the first expansion speed in LSI+61°303 that has been directly measured. This velocity is similar to expansion or ejection speeds measured for other well-studied X-ray binary systems (typically $\sim 0.15 - 0.3c$). As the flare decayed, this enlargement stopped; if the source had continued to extend, this increased size would have been clearly visible in our VLBI data for parts F1 and F2. The formal speed for parts D–F is $(0.006 \pm 0.006)c$, consistent with zero. The size of the source in the post-burst period (F1–F2) is ~ 2.0 mas and its flux is ~ 14 mJy. We do not know the reason for this apparent deceleration. One possibility could be that the mini-flare expanded into an evacuated cavity, but then ran into material from a more slowly expanding major ejection when it reached a dimension of ~ 2.0 mas. (Taylor et al., 1992 and Massi et al. 1993, report a size of about 2 mas some days after the peak of major outbursts).

4.2. Was the expanding source actually a double source?

In general, the picture described above –a uniformly expanding circular gaussian component on VLBI scales corresponding to the mini-flare detected with the VLA– fits the VLBI observations well. It gives a relatively simple, physically reasonable, and complete explanation of the observed changes in the VLBI source structure, within the constraints of the data available. Nonetheless, we have some evidence that the VLBI source structure may have been more complex, in particular, that it may have had a double structure. This evidence comes primarily from the VLBI data for part C, corresponding to the mini-flare maximum.

We had a relatively large number of VLBI data points for part C, and a relatively large number of intact closure triangles for the hybrid mapping. Model fitting indicates that a two-component model to this part data (with either points or gaussian components) renders a very good fit to both the amplitudes and

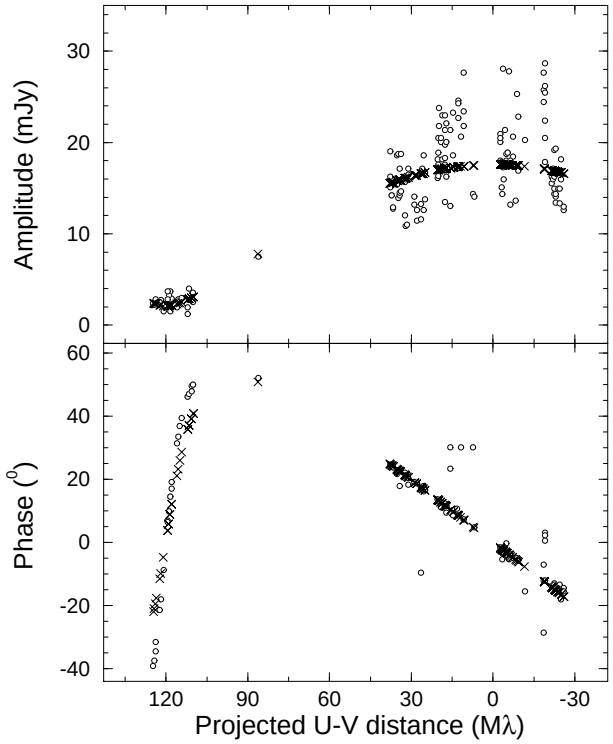

Fig. 8. Plots of the visibility phases and amplitudes for part C projected onto structural position angle –21°, together with the visibilities predicted by the best-fit point double model. The open circles represent the data and the crosses the model visibilities. The angle onto which the visibilities have been projected corresponds to the structural position angle for the point double model. The visibilities have also been shifted by a small amount so that the stronger component of the point double model is located at (0, 0).

phases. As an example, Fig. 8 shows the plots of the model and data visibility phases and amplitudes for part C for the best-fit model to two point components. We find that the double models clearly fit the visibility phases much better than the circular gaussian model. The double separation and total flux for the two–gaussian fit (1.3 mas and 19.8 mJy) are virtually identical to the size and total flux for the single circular gaussian fit to the amplitudes (1.2 mas and 21.3 mJy), giving us confidence that our analysis based on circular gaussian fitting of the visibility amplitudes renders reasonable estimates for the expansion speed of the VLBI source size during the mini-flare, even if the actual source structure may be more complex. This possibility also implies that the increasing size observed could correspond to a separation velocity of the components forming the complex structure.

We also tried to obtain double fits to the remaining datasets (A, B, D, E, F). For cases A and B the fits are satisfactory but do not significantly improve the circular gaussian fit. Case D behaves very similar to C: the two component models fit the visibility phases much better than the circular gaussian model. The alignment angle of the two components (–10.3°) slightly differs from case C, although this can be due to the different u-v coverages — and therefore, the directions of maximum resolution — for the different parts. The fact that we do not have closure phases for parts E and F does not allow us to obtain phase fits giving information about the orientation of possible elongated structure in the source.

In summary, although we cannot be sure whether the structure evolution for the compact radio emission of LSI+61°303 during the mini-flare was approximately spherically symmetric or occurred along a preferred direction, the data for parts C and D, for which we had the best coverage, suggest the latter.

5. Conclusions

We have detected roughly linear growth in size of the compact radio structure of LSI+61°303 during a "mini-flare" that occurred during our 24-hour VLBI observations. The velocity of structural enlargement is $v \sim 0.06c$, similar to the those observed in the radio emission of other X-ray binaries (and normally related with either expansion or plasmon ejection speeds) such as SS433 and Cyg X-3. The rather constant increase in size abruptly stops when the source reaches a dimension of ~ 2 mas (corresponding to about 4.5 AU at the distance of LSI+61°303. It at first seems puzzling that Taylor et al. (1992) and Massi et al. (1993) inferred speeds for major periodic outbursts roughly two orders of magnitude smaller than the speed reported here for a short amplitude flare. However, they used indirect arguments for their speed estimations, which assumed that the material they observed had been ejected some days before and had maintained a constant speed during these days. The slower velocities they inferred could be an average of much higher initial speeds that subsequently drastically decelerated, similar to the behavior for the smaller outburst we have analyzed here; it is also possible that the material seen by them had been ejected *after* the epoch they estimated.

These VLBI observations have shown that roughly 50–60% of the quiescent radio emission of LSI+61°303 is located on milli-arcsecond scales, with the remainder on scales intermediate between those sampled by the VLB interferometer and the VLA. The detection of compact (mas-scale) flaring radio emission in LSI+61°303 at an epoch that clearly is not near a major outburst peak indicates that between outbursts the radio emission of this source may have a different origin than during them, i.e., the "quiescent" radio emission of LSI+61°303 is not simply due to the slow decay of the radiation from the major outbursts. This is consistent with a scenario in which the inter-outburst flaring radio emission of LSI+61°303 is associated with the overlapping of series of small events, for example, from luminosity-driven shocks.

Acknowledgements. DCG acknowledges support from an American Astronomical Society Chretien Grant. MP acknowledges financial support from the Ministerio Español de Educación y Ciencia and partial support by DGICIT(PB94-0904)

References

Bignami G.F., Caraveo P.A., Lamb R.C., Markert T.H., Paul J.A., 1981, ApJ 247, L85
Cornwell T.J., Wilkinson P.N., 1981, MNRAS 196, 1067
Fichtel C.E., Bertsch D.L., Chiang J. et al. 1994, ApJS 94, 551
Gabuzda D.C., Roberts D.H., Wardle J.F.C., 1989, ApJ 338, 743
Gregory P.C., Taylor A.R., 1978, Nat 272, 704
Gregory P.C., Huang-Jian Xu, Backhouse C.J., Reid A., 1989, ApJ 339, 1054
Hermsem W., Swanenburg, B.N., Bignami G.F. et al. 1977, Nat 269, 495
Hjellming R.M., Johnston K.J., 1981, ApJ 246, L141
Hutchings J.B., Crampton D., 1981, PASP 93, 486
Lestrade J.-F., 1988, in *The Impact of VLBI on Astrophysics and Geophysics*, M.J. Reid and J.M. Moran Eds., Kluwer, Boston, 265
Maraschi L., Treves A., 1981, MNRAS 194, 18
Massi M., Paredes J.M., Estalella R., Felli M., 1993, A&A 269, 249
Mendelson H., Mazeh T., 1989, MNRAS 239, 733
Mendelson H., Mazeh T., 1994, MNRAS 267, 1
Mirabel I.F., Rodriguez L.F., 1994, Nat 371, 494
Molnar L.A., Reid M.J., Grindlay E.J., 1988, ApJ 331, 494
Paredes J.M., Estalella R., Rius A., 1990, A&A 232, 377
Paredes J.M., Marziani P., Martí J. et al. 1994, A&A 288, 512.
Peracaula M., Martí J., Paredes J.M., 1997, A&A in press
Roberts D.H., Lehar J., Dreher J.W. 1987, AJ 93, 968
Roberts D.H., Wardle J.F.C., Brown L.F., 1994, AJ 427, 718
Taylor A.R., Gregory P.C., 1982, ApJ 255, 210
Taylor A.R., Gregory P.C., 1984, ApJ 283, 273
Taylor A.R., Kenny H.T., Spencer R.E., Tzioumis A., 1992, ApJ 395, 268
Taylor A.R., Young G., Peracaula M., Kenny H.T., Gregory P.C., 1995, A&A 305, 817.
Verstrand W.T., 1983, ApJ 271, 304.
Waters L.B.F.M., Taylor A.R., van den Heuvel E.P.J., Habets G.M.H.J., Persi P., 1988, A&A 198, 200.

This article was processed by the author using Springer-Verlag LaTeX A&A style file *L-AA* version 3.